Published in final edited form as:
J Invest Dermatol. 2007 January ; 127(1): 16–23.

Loss of the acyl-CoA binding protein (Acbp) results in fatty acid metabolism abnormalities in mouse hair and skin

Lance Lee[1], **C. Anthony DeBono**[2], **Dean R. Campagna**[1], **David C. Young**[2], **D. Branch Moody**[2], and **Mark D. Fleming**[1]

1 *Department of Pathology, Children's Hospital Boston and Harvard Medical School, Boston, MA*

2 *Division of Rheumatology, Immunology and Allergy, Brigham and Women's Hospital and Harvard Medical School, Boston, MA*

Abstract

Proper fatty acid metabolism is critical for hair and skin development and maintenance. The acyl-CoA binding protein (Acbp) is a widely expressed protein that binds long-chain fatty acyl-CoA esters and plays a role in fatty acyl-CoA transport and pool formation. However, loss of function of Acbp in the whole animal has not been investigated. Here, we show that deletion of *Acbp* in mouse results in sebocyte hyperplasia and sparse, matted hair with a greasy appearance. Consistent with these gross abnormalities, *Acbp* is highly expressed in the pilosebaceous units of mouse skin as determined by northern analysis and *in situ* hybridization. Loss of *Acbp* also results in fatty acid metabolism abnormalities, with hair lipid profiles showing altered levels of triacylglycerols and nearly co-migrating lipids. These data suggest that Acbp plays a role in triacylglycerol biosynthesis and that regulation of this process is important for proper hair and skin development and maintenance in the mouse.

INTRODUCTION

Long-chain fatty acyl-CoA esters function as substrates and intermediates in lipid biosynthesis and catabolism and also play a role in regulating carbohydrate metabolism, protein sorting, gene expression, and signal transduction (Faergeman and Knudsen, 1997; Knudsen *et al.*, 2000). Homeostatic control of these molecules is therefore essential for numerous cellular functions.

The acyl-CoA binding protein (Acbp), which was also identified as the diazepam binding inhibitor (Mocchetti and Santi, 1991), is a 10 kD, cytoplasmic protein that binds medium- and long-chain fatty acyl-CoA esters and plays a role in fatty acid metabolism (Knudsen *et al.*, 1999). Acbp is found in eukaryotes ranging from yeast to mammals (Knudsen *et al.*, 1999). Although testis- and brain-specific isoforms have been identified, most tissues express a common form (Knudsen *et al.*, 1999).

Several studies have indicated that Acbp contributes to intracellular acyl-CoA transport and pool formation. *In vitro*, Acbp binds C_{14}-C_{22} acyl-CoA esters with high affinity but does not bind free fatty acids, acyl carnitines, or cholesterol (Rasmussen *et al.*, 1990; Rosendal *et al.*, 1993). Acbp protects long-chain acyl-CoA esters from hydrolysis by microsomal hydrolases

CORRESPONDING AUTHOR: Mark D. Fleming, Department of Pathology, Enders 1116, Children's Hospital Boston, 300 Longwood Avenue, Boston, MA 02115. Phone: (617) 919-2664. Fax: (617) 730-0168. E-mail: mark.fleming@childrens.harvard.edu..

CONFLICT OF INTEREST

The authors declare no conflict of interest.

LOCATION OF WORK: Boston, Massachusetts, USA

and can donate acyl-CoA for mitochondrial oxidation and microsomal glycerolipid synthesis (Rasmussen *et al*., 1994; Rasmussen *et al*., 1993). Specifically, *in vitro*, binding of long-chain fatty acyl-CoAs to Acbp inhibits their incorporation into triacylglycerols in microsomal membranes, whereas incorporation into phospholipids is relatively unaffected, suggesting that Acbp preferentially donates fatty acyl-CoAs for neutral glycerolipid synthesis (Rasmussen *et al.*, 1993). Over-expression of the bovine or *Saccharomyces cerevisiae* orthologs in yeast results in an increase in the intracellular acyl-CoA ester pool size (Mandrup *et al.*, 1993; Schjerling *et al.*, 1996). Conversely, disruption of the yeast ortholog results in an accumulation of long-chain acyl-CoA esters, particularly octadecanoyl-CoA (C18:0), with no change in fatty acyl-CoA synthesis (Schjerling *et al.*, 1996). Addition of Acbp causes a dramatic decrease in the average chain length of acyl-CoA esters, suggesting that Acbp may function in transport of acyl-CoA esters from the site of synthesis to the intracellular pools where they are available for enzymes involved in their processing and catabolism. Overall, these studies indicate that Acbp plays a role in the availability of long-chain fatty acyl-CoA esters for a variety of biochemical processes.

To date, most Acbp functional studies have been performed *in vitro* or in yeast. Reduction of Acbp in a variety of human cell lines by small interference RNA results in cell lethality, suggesting that Acbp performs an essential function (Faergeman and Knudsen, 2002). Recently, transgenic over-expression of *Acbp* in mice was shown to result in an increase in liver long-chain fatty acyl-CoA pool size, particularly levels of saturated and polyunsaturated fatty acyl-CoAs (Huang *et al.*, 2005). However, loss of function has not been investigated *in vivo*.

In this paper, we describe hair and skin abnormalities in mice homozygous for the *nm1054* mutation, which was previously described as a recessive, pleiotropic mutation caused by an approximately 400 kb deletion on chromosome 1 (Ohgami *et al.*, 2005a; Ohgami *et al.*, 2005b). Here, we characterize hair and skin abnormalities in *nm1054* deletion mutants and show that these phenotypes result from a loss of *Acbp* and are related to a defect in cutaneous fatty acid metabolism.

RESULTS

Cutaneous abnormalities in *nm1054* mice

As they develop their adult coat, B6129F1 mice homozygous for the *nm1054* deletion have sparse, reddish, matted hair with a greasy appearance (Figure 1a–c). To determine the nature of the cutaneous abnormality, we examined the histological appearance of adult skin from a variety of locations. The epidermis and dermis appear normal in *nm1054* mutants, and there is a normal distribution of pilosebaceous units (PSUs), which are comprised of hair follicles and sebocytes. However, consistent with the greasy appearance of *nm1054* hair, there is an increased number of sebocytes associated with most PSUs from skin of the lower thorax (Figure 2a–b) and the nose (Figure 2c–d) of *nm1054* deletion homozygotes. No differences were observed in the skin from the paws (Figure 2e–f) or the tail (Figure 2g–h), or in juvenile skin (data not shown).

Transgenic rescue of the cutaneous phenotype

A BAC contig of the *nm1054* deletion interval was developed previously (Ohgami *et al.*, 2005b). Two transgenic lines derived from CITB BAC clone 486B9 (Kim *et al.*, 1996) rescue the gross and microscopic cutaneous phenotypes but not the other *nm1054* phenotypes (Figure 3a–c; (Ohgami *et al.*, 2005a). Based on sequence analysis, two genes are predicted to be present on BAC 486B9: *Acbp* and a novel gene, which will be referred to by its GenBank accession number *BAB29121* (Carninci and Hayashizaki, 1999). The appearance of the hair and the

sebocyte hyperplasia in deletion mutants, combined with the documented role of Acbp in fatty acid metabolism, suggested that *Acbp* was a strong candidate for the *nm1054* cutaneous phenotype.

The *BAB29121* gene has five exons and encodes a novel, 121 amino acid predicted protein with no identifiable domains and no homology to any known proteins. ESTs have been sequenced from thymus, uterus, mammary gland, lymph node, and brain, and there are predicted orthologs in species ranging from yeast to humans. *BAB29121* is expressed in wild type mouse thymus but not in *nm1054* or BAC 486B9 transgenic *nm1054* animals (Figure 3d), suggesting that the gene or regulatory elements may extend beyond the limits of the BAC or are disrupted by insertion of circularized BAC DNA. Alternatively, the gene could be silenced due to a positional insertion effect. Lack of *BAB29121* expression in BAC 486B9 transgenic *nm1054* animals further suggests that the cutaneous phenotypes result solely from a loss of *Acbp*.

Expression of *Acbp*

Acbp expression was previously documented in murine brain, liver and kidney by northern analysis (Owens *et al.*, 1989). Expression of the rat and bovine orthologs has also been reported in many tissues (Bovolin *et al.*, 1990; Mikkelsen and Knudsen, 1987; Mocchetti *et al.*, 1986). A murine northern blot shows strong *Acbp* expression in most tissues, with the highest expression in liver and skin and lower levels in spleen, muscle, and thymus (Figure 4a).

Because of the abnormalities in *nm1054* skin and the high level of *Acbp* expression in skin by northern analysis, we performed *in situ* hybridization for *Acbp* mRNA. *Acbp* expression was detected in the epidermis, hair follicles, and sebocytes of skin from the lower thorax (Figure 4b). This finding is consistent with ACBP protein expression in the epidermis and sebaceous glands of human skin (Alho *et al.*, 1993). Similar epidermal and PSU expression was detected in skin from the nose (Figure 4d). No expression was detected in *nm1054* skin (Figure 4c,e). Taken together with the function of Acbp in lipid metabolism and the absence of *BAB29121* expression in BAC transgenic *nm1054* mutants, these data provide further evidence that *Acbp* is responsible for the *nm1054* hair and skin abnormalities.

Lipid analysis in *nm1054* mice

Since *in vitro* studies had previously implicated Acbp in binding and metabolism of acyl-CoA esters, as well as facilitating production of various acylated lipids, we carried out global lipid analyses in several tissues from wild type, *nm1054*, and BAC 486B9 transgenic *nm1054* mice. We used multiple methods to develop complete profiles for lipids from liver, skin, and hair. Although we detected no differences in the profiles of liver or skin lipids (Figure S1, Figure S2, and data not shown), distinctive differences were observed in the profile of lipids extracted from hair.

Silica thin layer chromatography (TLC) and high performance liquid chromatography-mass spectrometry (HPLC-MS) demonstrated no significant differences in the levels of most major classes of polar and non-polar hair lipids from wild type, *nm1054*, and BAC 486B9 transgenic *nm1054* mice (Figure 5a, Figure S1, Figure S2, data not shown). However, we reproducibly observed a band unique to *nm1054* hair and a species present in all three genotypes that was reduced in relative intensity in the *nm1054* mutant (Figure 5a). Based on the similar migration of the common and unique bands, we inferred that these were likely structurally related lipids and attempted to identify both using an extensive battery of methods. The band unique to *nm1054* did not give strong ions in mass spectrometry, and we were unable to obtain sufficient amounts to obtain a coherent nuclear magnetic resonance spectrum (data not shown). Consequently, we were unable to identify its structure. However, commensurate with its co-

migration with the triacylglycerol standard tristearin (Figure 5a), positive mode mass spectrometry in the presence of lithium revealed that the common band represents triacylglycerols, with the strongest ion of m/z 865.7 corresponding to the expected mass of a lithium adduct of a triacylglycerol with a total fatty acyl chain length of C_{52} and two unsaturations (Figure 5b). Collision-induced mass spectrometry identified ions corresponding to products derived from the loss of $C_{18:1}$ and $C_{16:0}$ fatty acyl chains, confirming the identity of this lipid (Figure 5c). Overall, these data indicate that *nm1054* mice produce sebaceous lipids with reduced levels of triacylglycerols accompanied by the appearance of an unidentified, nearly co-migrating lipid.

DISCUSSION

In this study, we have uncovered an important role for the acyl-CoA binding protein in mouse hair and skin. We have demonstrated that the gene encoding the acyl-CoA binding protein is expressed at high levels in the pilosebaceous units of mouse skin and that loss of *Acbp* is responsible for the abnormal cutaneous phenotype of *nm1054* mice. Consistent with the reported role of Acbp in lipid metabolism and its preferential role in synthesis of neutral glycerolipids, we identified a selective abnormality in triacylglycerols present on *nm1054* hair.

Acbp joins a growing list of fatty acid metabolism genes in which mutations result in selective or predominant cutaneous phenotypes. Among these proteins is fatty acid transport protein 4 (Fatp4), which functions as an acyl-CoA synthetase and plays an important role in uptake and metabolism of long and very long chain fatty acids (Hall *et al.*, 2005; Hirsch *et al.*, 1998; Stahl *et al.*, 1999). Loss of *Fatp4* results in neonatal lethality due to restrictive dermopathy, a condition characterized by abnormally thin and tight skin with an expanded epidermis, a restricted dermis, and a reduced number of PSUs (Herrmann *et al.*, 2003; Moulson *et al.*, 2003). Similarly, Elovl3 belongs to a family of enzymes involved in the biosynthesis of very long chain fatty acids (Tvrdik *et al.*, 2000) and is expressed primarily in the sebaceous glands and hair follicles of the skin (Westerberg *et al.*, 2004). Mice deficient for *Elovl3* have sparse fur, an expanded epidermis, and enlarged sebocytes (Westerberg *et al.*, 2004). Loss of the gene encoding the acyl-CoA:diacylglycerol acyltransferase, a key enzyme in diacylglycerol synthesis, results in sparse, dry hair and a decreased number of sebocytes (Chen *et al.*, 2002). Mice lacking stearoyl-CoA desaturase, which is involved in monounsaturated fatty acid biosynthesis, have atrophic sebocytes and a decreased level of triglycerides and cholesterol esters in the skin (Miyazaki *et al.*, 2001). Finally, sparse hair and cyst-like inclusions in the skin of *scraggly* mice result from an abnormal lipid distribution in the hair and skin (Herron *et al.*, 1999). These studies, along with our own, indicate that proper fatty acid metabolism is critical for normal hair and skin development and maintenance.

Acbp is thought to bind medium- and long-chain fatty acyl-CoA esters and donate them for use in other processes, including triacylglycerol biosynthesis (Rasmussen *et al.*, 1994; Rasmussen *et al.*, 1993). TLC analysis shows that *nm1054* hair has a relative decrease in triacylglycerols and an accompanying increase in a novel, closely migrating band that may represent a related lipid, suggesting a defect in triacylglycerol metabolism. Despite extensive characterization, we were unable to identify the novel lipid under conditions where common lipids were readily detected (Figure 5b; data not shown).

The increase in sebocytes and the altered lipid profile undoubtedly contribute to the matted, greasy appearance of the adult coat. It is possible that the sebocyte hyperplasia itself is due to an increase in peroxisome proliferator-activated receptor (PPAR)-mediated gene transcription. The PPARs are nuclear hormone receptors that are activated by binding to fatty acids (Forman *et al.*, 1997; Kliewer *et al.*, 1997; Krey *et al.*, 1997) and regulate transcription of a plethora of genes involved in lipid metabolism (Gervois *et al.*, 2000; Kota *et al.*, 2005; Smith, 2002) and

skin development (Di-Poi *et al.*, 2004; Rosenfield *et al.*, 2000). Loss of the gene encoding the PPARγsubtype is embryonic lethal (Rosen *et al.*, 1999). However, analysis of chimeric PPARγ null mice showed that PPARγ is required for sebocyte differentiation. Furthermore, expression of PPARγ in cultured cells promotes sebocyte maturation, lipid accumulation, and triacylglycerol synthesis (Rosenfield *et al.*, 1999; Schadinger *et al.*, 2005).

Consistent with the role of PPARγ in sebocyte differentiation, PPARγ and Acbp may function interdependently in fatty acid metabolism. *Acbp* and PPARγ are both expressed in the epidermis, hair follicles, and sebocytes of mouse skin (Figure 4; (Di-Poi *et al.*, 2004;Rosenfield *et al.*, 2000), and these cell lineages share a common origin and can affect differentiation and function of one another (Ferraris *et al.*, 1997;Oshima *et al.*, 2001;Reynolds and Jahoda, 1992;Taylor *et al.*, 2000). Acbp is up-regulated by PPARγ and is thought to compete for binding to fatty acids that stimulate PPARγ-dependent transcription (Helledie *et al.*, 2000;Helledie *et al.*, 2002a). The processes of fatty acid conversion to CoA esters and reversion back to free fatty acids are in constant equilibrium, with CoA esters preferentially binding Acbp and free fatty acids binding PPARγ (Helledie *et al.*, 2002b;Hertz *et al.*, 1994;Hunt *et al.*, 1999). An increase in Acbp expression or an increase in the level of fatty acyl-CoA esters decreases PPARγ-mediated transcription, presumably by reducing the level of free fatty acids available for binding to PPARγ (Helledie *et al.*, 2000;Helledie *et al.*, 2002a). Therefore, in the absence of Acbp, fatty acids may be in excess and available to stimulate PPARγ-mediated transcription, which could eventuate into sebocyte hyperplasia and alterations in hair lipid composition. Alternatively, it is entirely possible that changes in triacylglycerol metabolism may regulate transcription of other signals in a PPAR-independent manner.

Although *Acbp* is expressed in all tissues, we did not detect morphological or lipid abnormalities in any tissue other than hair or skin. To this end, there may be proteins functionally redundant with Acbp, and expression of these molecules may vary in different tissues. This possibility could also explain the difference between yeast with a targeted deletion of the *Acbp* ortholog, where there is a dramatic increase in long-chain fatty acyl-CoA esters (Schjerling *et al.*, 1996), and *nm1054* mouse hair, where the vast majority of lipids are synthesized at normal levels and have correct fatty acyl chain lengths. Alternatively, it is possible that loss of *Acbp* produces a cell-autonomous defect in mouse skin, whereas other tissues may compensate for a loss of *Acbp* by taking up lipids or other molecules produced elsewhere through redundant pathways. Such molecules may not be in sufficient supply in skin, necessitating the requirement for endogenous Acbp. This hypothesis could explain the apparently paradoxical findings that *Acbp* is essential in cell culture (Faergeman and Knudsen, 2002) and the whole animal lacking the gene survives.

At the present time, no human disorders have been described that resemble the hair and skin phenotype seen in *nm1054* mice, and no related lipid metabolism disorders have been mapped near *ACBP*. However, an increased understanding of the role of Acbp in cutaneous development and maintenance could play a pivotal role in future studies of human skin disease pathophysiology and therapy.

MATERIALS AND METHODS

Mice

The *nm1054* mutation was maintained on both the C57BL/6J (B6) and the 129S6/SvEvTac (129) backgrounds as previously described (Ohgami *et al.*, 2005a). All phenotypic analysis was performed on B6129F1 males at 8 or 24 weeks. All animal procedures were approved by the Animal Care and Use Committee at Children’s Hospital Boston.

Transgenic rescue

BAC transgenic animals were generated as previously described (Ohgami *et al.*, 2005b). Transgenic mice were identified by BAC end-specific PCR, as well as internal polymorphisms between the 129X1/SvJ transgene and the C57BL/6 background.

Histological analysis

Eight- and 24-week-old mice were euthanized, and the entire pelt and the ears were fixed in 10% buffered formalin. After 24 hours, the nose and standardized sections of skin from the lower thorax were transferred to 70% ethanol. Paws and tails were fixed in Bouin's fixative until the bones were fully decalcified. All tissues were embedded in paraffin, sectioned, and stained with hematoxylin and eosin.

Northern analysis

A ^{32}P-labeled *Acbp* probe was generated by PCR amplification of the open reading frame from EST clone BQ947297 (Invitrogen, Carlsbad, CA), which contains full-length *Acbp*, using primers 5'- CCTCAAGACTCAGCCAACTG-3' and 5'-GACTCGTGGAACAAGCTGAA-3'. A multi-tissue mouse northern blot (OriGene Technologies, Inc., Rockville, MD) was prehybridized in MiracleHyb solution (Stratagene, La Jolla, CA) for 30 minutes at 65^{o}C and hybridized in the same solution with the *Acbp* probe. The blot was washed twice with 2X SSC / 0.1% SDS and then twice with 0.2X SSC / 0.1% SDS, all at 65^{o}C. Expression was detected by autoradiography.

In situ hybridization

Ten micrograms of EST clone BQ947297 (Invitrogen, Carlsbad, CA) were digested with *SalI* and *HindIII* to generate antisense and sense probes, respectively. Riboprobes were labeled using a digoxigenin RNA labeling kit (Roche Molecular Biochemicals, Indianapolis, IN). Automated *in situ* hybridization was performed on the Ventana Discovery System (Ventana Medical Systems, Tucson, AZ). Wild type and *nm1054* skin were fixed in 4% paraformaldehyde and embedded in paraffin. Deparaffinized sections were digested with proteinase K at 37^{o}C, hybridized at 65^{o}C for 6 hours, and washed twice in 0.1X SSC at 75^{o}C. The digoxigenin label was detected with a biotinylated anti-digoxigenin antibody (Biogenex, San Ramon, CA), followed by a streptavidin-alkaline phosphatase conjugate, and visualized by an NBT/BCIP substrate reaction with the BlueMap Detection Kit (Ventana Medical Systems, Tucson, AZ). Slides were counterstained with nuclear fast red (Vector Laboratories, Inc., Burlingame, CA), dehydrated, and analyzed by light microscopy.

RT PCR

RNA was isolated from mouse thymus using the RNAqueous kit (Ambion, Austin, TX). 0.5μg RNA was primed with an oligo-dT primer and reverse transcribed using the SuperScript first strand synthesis kit (Invitrogen, Carlsbad, CA). *BAB29121* was amplified from reverse transcribed cDNA using primers 5'-CTCATCCGTTCATTTGAGCA-3' and 5'-CAGGACGAGATGGGATTAGC-3'. Amplification products were visualized by agarose gel electrophoresis.

Lipid isolation

Lipids were derived from plucked fur, sections of shaved skin, and sections of liver from eight- and 24-week old male mice fasted for four hours. Lipids were extracted serially with choloform:methanol 2:1 (v/v), chloroform:methanol 1:1, and chloroform:methanol 1:2, each for one hour at room temperature. After each extraction, the samples were centrifuged at 2,000

X g for five minutes. The supernatants containing the lipids were pooled, evaporated under a nitrogen stream, and solvated in cholorform.

Thin layer chromatography

Polar and non-polar lipids were separated by thin layer chromatography (TLC) using silica plates (Scientific Adsorbents, Inc., Atlanta, GA). Equal amounts of lipids extracted from plucked hair, skin, or liver of wild type, *nm1054*, and BAC 486B9 transgenic *nm1054* mice were spotted onto TLC plates. For polar lipids, plates were developed with chloroform:methanol:water 60:35:5 (v/v/v). Non-polar lipids were separated and analyzed as previously described (Downing, 1968). Briefly, after development with hexane to the top of the plate, the plate was dried, redeveloped to the same point with benzene, dried, and developed again with hexane:diethyl ether:acetic acid 70:30:1 (v/v/v) to the midpoint of the plate. TLC bands were visualized either by spraying the plate with 3% cupric acetate (w/v) in 8% phosphoric acid (v/v), followed by charring at 180^{o}C, or by a non-destructive method modified from Plekhanov (Plekhanov, 1999). Briefly, the plate was sprayed with 1M ammonium acetate and then submerged in a 1M ammonium acetate solution saturated with naphthol blue black (Sigma-Aldrich, St. Louis, MO) and dried. Bands were scraped and extracted three times with 5 ml chloroform:methanol 2:1 (v/v).

High performance liquid chromatography – mass spectrometry

Equal amounts of polar lipids were separated by high performance liquid chromatography – mass spectrometry using a method modified from Matsunaga et al. (Matsunaga *et al.*, 2004). A Monochrome Diol column was coupled online to an LCQ Advantage ion-trap mass spectrometer equipped with an electrospray ionization source. Mobile phase A was hexane:isopropanol 60:40 (v/v) containing 0.1% formic acid, 0.05% ammonium hydroxide, and 0.05% triethylamine. Mobile phase B was methanol containing 0.1% formic acid, 0.05% ammonium hydroxide, and 0.05% triethylamine. Using a flow rate of 0.7 ml/minute, a binary gradient started at 5% mobile phase B (B), increased linearly to 15% B in six minutes, held for 10 minutes, increased linearly to 100% B in 12 minutes, held for six minutes, and returned to 5% B in two minutes. Eluants were analyzed by UV absorbance and direct online mass spectrometry.

Supplementary Material

Refer to Web version on PubMed Central for supplementary material.

Acknowledgements

We gratefully thank James Edwards and Tonora Archibald in the Pathology Department's histology core facility at Children's Hospital Boston, as well as Yu Yang in the Dana Farber – Partners Cancer Center *in situ* core facility, for their technical assistance and expertise. We also thank Nancy Andrews and members of the Andrews and Fleming labs for their ongoing suggestions. This work was supported by the Pew Foundation Scholars in the Biomedical Sciences Program (M.D.F. and D.B.M.), the Mizutani Foundation for Glycoscience (D.B.M.), and the National Institutes of Health (HL074247 for M.D.F. and AR48632 and AI49313 for D.B.M.). L.L. was supported in part by an NIH postdoctoral NRSA training grant (HL007574.23).

References

Alho H, Vaalasti A, Podkletnova I, Rechardt L. Expression of diazepam-binding inhibitor peptide in human skin: an immunohistochemical and ultrastructural study. J Invest Dermatol 1993;101:800–3. [PubMed: 8245508]

Bovolin P, Schlichting J, Miyata M, Ferrarese C, Guidotti A, Alho H. Distribution and characterization of diazepam binding inhibitor (DBI) in peripheral tissues of rat. Regul Pept 1990;29:267–81. [PubMed: 2171047]

Carninci P, Hayashizaki Y. High-efficiency full-length cDNA cloning. Methods Enzymol 1999;303:19–44. [PubMed: 10349636]

Chen HC, Smith SJ, Tow B, Elias PM, Farese RV Jr. Leptin modulates the effects of acyl CoA:diacylglycerol acyltransferase deficiency on murine fur and sebaceous glands. J Clin Invest 2002;109:175–81. [PubMed: 11805129]

Di-Poi N, Michalik L, Desvergne B, Wahli W. Functions of peroxisome proliferator-activated receptors (PPAR) in skin homeostasis. Lipids 2004;39:1093–9. [PubMed: 15726824]

Downing DT. Photodensitometry in the thin-layer chromatographic analysis of neutral lipids. J Chromatogr 1968;38:91–9. [PubMed: 5688076]

Faergeman NJ, Knudsen J. Role of long-chain fatty acyl-CoA esters in the regulation of metabolism and in cell signalling. Biochem J 1997;323 :1–12. [PubMed: 9173866]Pt 1

Faergeman NJ, Knudsen J. Acyl-CoA binding protein is an essential protein in mammalian cell lines. Biochem J 2002;368:679–82. [PubMed: 12396232]

Ferraris C, Bernard BA, Dhouailly D. Adult epidermal keratinocytes are endowed with pilosebaceous forming abilities. Int J Dev Biol 1997;41:491–8. [PubMed: 9240566]

Forman BM, Chen J, Evans RM. Hypolipidemic drugs, polyunsaturated fatty acids, and eicosanoids are ligands for peroxisome proliferator-activated receptors alpha and delta. Proc Natl Acad Sci U S A 1997;94:4312–7. [PubMed: 9113986]

Gervois P, Torra IP, Fruchart JC, Staels B. Regulation of lipid and lipoprotein metabolism by PPAR activators. Clin Chem Lab Med 2000;38:3–11. [PubMed: 10774955]

Hall AM, Wiczer BM, Herrmann T, Stremmel W, Bernlohr DA. Enzymatic properties of purified murine fatty acid transport protein 4 and analysis of acyl-CoA synthetase activities in tissues from FATP4 null mice. J Biol Chem 2005;280:11948–54. [PubMed: 15653672]

Helledie T, Antonius M, Sorensen RV, Hertzel AV, Bernlohr DA, Kolvraa S, et al. Lipid-binding proteins modulate ligand-dependent trans-activation by peroxisome proliferator-activated receptors and localize to the nucleus as well as the cytoplasm. J Lipid Res 2000;41:1740–51. [PubMed: 11060343]

Helledie T, Grontved L, Jensen SS, Kiilerich P, Rietveld L, Albrektsen T, et al. The gene encoding the Acyl-CoA-binding protein is activated by peroxisome proliferator-activated receptor gamma through an intronic response element functionally conserved between humans and rodents. J Biol Chem 2002a;277:26821–30. [PubMed: 12015306]

Helledie T, Jorgensen C, Antonius M, Krogsdam AM, Kratchmarova I, Kristiansen K, et al. Role of adipocyte lipid-binding protein (ALBP) and acyl-coA binding protein (ACBP) in PPAR-mediated transactivation. Mol Cell Biochem 2002b;239:157–64. [PubMed: 12479581]

Herrmann T, van der Hoeven F, Grone HJ, Stewart AF, Langbein L, Kaiser I, et al. Mice with targeted disruption of the fatty acid transport protein 4 (Fatp 4, Slc27a4) gene show features of lethal restrictive dermopathy. J Cell Biol 2003;161:1105–15. [PubMed: 12821645]

Herron BJ, Bryda EC, Heverly SA, Collins DN, Flaherty L. Scraggly, a new hair loss mutation on mouse chromosome 19. Mamm Genome 1999;10:864–9. [PubMed: 10441736]

Hertz R, Berman I, Bar-Tana J. Transcriptional activation by amphipathic carboxylic peroxisomal proliferators is induced by the free acid rather than the acyl-CoA derivative. Eur J Biochem 1994;221:611–5. [PubMed: 8168549]

Hirsch D, Stahl A, Lodish HF. A family of fatty acid transporters conserved from mycobacterium to man. Proc Natl Acad Sci U S A 1998;95:8625–9. [PubMed: 9671728]

Huang H, Atshaves BP, Frolov A, Kier AB, Schroeder F. Acyl-coenzyme a binding protein expression alters liver fatty acyl-coenzyme a metabolism. Biochemistry 2005;44:10282–97. [PubMed: 16042405]

Hunt MC, Nousiainen SE, Huttunen MK, Orii KE, Svensson LT, Alexson SE. Peroxisome proliferator-induced long chain acyl-CoA thioesterases comprise a highly conserved novel multi-gene family involved in lipid metabolism. J Biol Chem 1999;274:34317–26. [PubMed: 10567408]

Kim UJ, Birren BW, Slepak T, Mancino V, Boysen C, Kang HL, et al. Construction and characterization of a human bacterial artificial chromosome library. Genomics 1996;34:213–8. [PubMed: 8661051]

Kliewer SA, Sundseth SS, Jones SA, Brown PJ, Wisely GB, Koble CS, et al. Fatty acids and eicosanoids regulate gene expression through direct interactions with peroxisome proliferator-activated receptors alpha and gamma. Proc Natl Acad Sci U S A 1997;94:4318–23. [PubMed: 9113987]

Knudsen J, Jensen MV, Hansen JK, Faergeman NJ, Neergaard TB, Gaigg B. Role of acylCoA binding protein in acylCoA transport, metabolism and cell signaling. Mol Cell Biochem 1999;192:95–103. [PubMed: 10331663]

Knudsen J, Neergaard TB, Gaigg B, Jensen MV, Hansen JK. Role of acyl-CoA binding protein in acyl-CoA metabolism and acyl-CoA-mediated cell signaling. J Nutr 2000;130:294S–8S. [PubMed: 10721891]

Kota BP, Huang TH, Roufogalis BD. An overview on biological mechanisms of PPARs. Pharmacol Res 2005;51:85–94. [PubMed: 15629253]

Krey G, Braissant O, L'Horset F, Kalkhoven E, Perroud M, Parker MG, et al. Fatty acids, eicosanoids, and hypolipidemic agents identified as ligands of peroxisome proliferator-activated receptors by coactivator-dependent receptor ligand assay. Mol Endocrinol 1997;11:779–91. [PubMed: 9171241]

Mandrup S, Jepsen R, Skott H, Rosendal J, Hojrup P, Kristiansen K, et al. Effect of heterologous expression of acyl-CoA-binding protein on acyl-CoA level and composition in yeast. Biochem J 1993;290 :369–74. [PubMed: 8452523]Pt 2

Matsunaga I, Bhatt A, Young DC, Cheng TY, Eyles SJ, Besra GS, et al. Mycobacterium tuberculosis pks12 produces a novel polyketide presented by CD1c to T cells. J Exp Med 2004;200:1559–69. [PubMed: 15611286]

Mikkelsen J, Knudsen J. Acyl-CoA-binding protein from cow. Binding characteristics and cellular and tissue distribution. Biochem J 1987;248:709–14. [PubMed: 3435479]

Miyazaki M, Man WC, Ntambi JM. Targeted disruption of stearoyl-CoA desaturase1 gene in mice causes atrophy of sebaceous and meibomian glands and depletion of wax esters in the eyelid. J Nutr 2001;131:2260–8. [PubMed: 11533264]

Mocchetti I, Einstein R, Brosius J. Putative diazepam binding inhibitor peptide: cDNA clones from rat. Proc Natl Acad Sci U S A 1986;83:7221–5. [PubMed: 3463960]

Mocchetti I, Santi MR. Diazepam binding inhibitor peptide: cloning and gene expression. Neuropharmacology 1991;30:1365–71. [PubMed: 1780035]

Moulson CL, Martin DR, Lugus JJ, Schaffer JE, Lind AC, Miner JH. Cloning of wrinkle-free, a previously uncharacterized mouse mutation, reveals crucial roles for fatty acid transport protein 4 in skin and hair development. Proc Natl Acad Sci U S A 2003;100:5274–9. [PubMed: 12697906]

Ohgami RS, Campagna DR, Antiochos B, Wood EB, Sharp JJ, Barker JE, et al. nm1054, a spontaneous, recessive, hypochromic, microcytic anemia mutation in the mouse. Blood 2005a;106:3625–31. [PubMed: 15994289]

Ohgami RS, Campagna DR, Greer EL, Antiochos B, McDonald A, Chen J, et al. Identification of a ferrireductase required for efficient transferrin-dependent iron uptake in erythroid cells. Nat Genet 2005b;37:1264–9. [PubMed: 16227996]

Oshima H, Rochat A, Kedzia C, Kobayashi K, Barrandon Y. Morphogenesis and renewal of hair follicles from adult multipotent stem cells. Cell 2001;104:233–45. [PubMed: 11207364]

Owens GP, Sinha AK, Sikela JM, Hahn WE. Sequence and expression of the murine diazepam binding inhibitor. Brain Res Mol Brain Res 1989;6:101–8. [PubMed: 2615592]

Plekhanov AY. Rapid staining of lipids on thin-layer chromatograms with amido black 10B and other water-soluble stains. Anal Biochem 1999;271:186–7. [PubMed: 10419634]

Rasmussen JT, Borchers T, Knudsen J. Comparison of the binding affinities of acyl-CoA-binding protein and fatty-acid-binding protein for long-chain acyl-CoA esters. Biochem J 1990;265:849–55. [PubMed: 2306218]

Rasmussen JT, Faergeman NJ, Kristiansen K, Knudsen J. Acyl-CoA-binding protein (ACBP) can mediate intermembrane acyl-CoA transport and donate acyl-CoA for beta-oxidation and glycerolipid synthesis. Biochem J 1994;299 :165–70. [PubMed: 8166635]Pt 1

Rasmussen JT, Rosendal J, Knudsen J. Interaction of acyl-CoA binding protein (ACBP) on processes for which acyl-CoA is a substrate, product or inhibitor. Biochem J 1993;292 :907–13. [PubMed: 8318018]Pt 3

Reynolds AJ, Jahoda CA. Cultured dermal papilla cells induce follicle formation and hair growth by transdifferentiation of an adult epidermis. Development 1992;115:587–93. [PubMed: 1425341]

Rosen ED, Sarraf P, Troy AE, Bradwin G, Moore K, Milstone DS, et al. PPAR gamma is required for the differentiation of adipose tissue in vivo and in vitro. Mol Cell 1999;4:611–7. [PubMed: 10549292]

Rosendal J, Ertbjerg P, Knudsen J. Characterization of ligand binding to acyl-CoA-binding protein. Biochem J 1993;290 :321–6. [PubMed: 7680855]Pt 2

Rosenfield RL, Deplewski D, Greene ME. Peroxisome proliferator-activated receptors and skin development. Horm Res 2000;54:269–74. [PubMed: 11595816]

Rosenfield RL, Kentsis A, Deplewski D, Ciletti N. Rat preputial sebocyte differentiation involves peroxisome proliferator-activated receptors. J Invest Dermatol 1999;112:226–32. [PubMed: 9989800]

Schadinger SE, Bucher NL, Schreiber BM, Farmer SR. PPARgamma2 regulates lipogenesis and lipid accumulation in steatotic hepatocytes. Am J Physiol Endocrinol Metab 2005;288:E1195–205. [PubMed: 15644454]

Schjerling CK, Hummel R, Hansen JK, Borsting C, Mikkelsen JM, Kristiansen K, et al. Disruption of the gene encoding the acyl-CoA-binding protein (ACB1) perturbs acyl-CoA metabolism in Saccharomyces cerevisiae. J Biol Chem 1996;271:22514–21. [PubMed: 8798418]

Smith SA. Peroxisome proliferator-activated receptors and the regulation of mammalian lipid metabolism. Biochem Soc Trans 2002;30:1086–90. [PubMed: 12440979]

Stahl A, Hirsch DJ, Gimeno RE, Punreddy S, Ge P, Watson N, et al. Identification of the major intestinal fatty acid transport protein. Mol Cell 1999;4:299–308. [PubMed: 10518211]

Taylor G, Lehrer MS, Jensen PJ, Sun TT, Lavker RM. Involvement of follicular stem cells in forming not only the follicle but also the epidermis. Cell 2000;102:451–61. [PubMed: 10966107]

Tvrdik P, Westerberg R, Silve S, Asadi A, Jakobsson A, Cannon B, et al. Role of a new mammalian gene family in the biosynthesis of very long chain fatty acids and sphingolipids. J Cell Biol 2000;149:707–18. [PubMed: 10791983]

Westerberg R, Tvrdik P, Unden AB, Mansson JE, Norlen L, Jakobsson A, et al. Role for ELOVL3 and fatty acid chain length in development of hair and skin function. J Biol Chem 2004;279:5621–9. [PubMed: 14581464]

ABBREVIATIONS

Acbp
: Acyl-CoA binding protein

B6
: C57BL/6J

129
: 129S6/SvEvTac

PSU
: pilosebaceous unit

TLC
: thin-layer chromatography

PPAR
: peroxisome proliferator-activated receptor

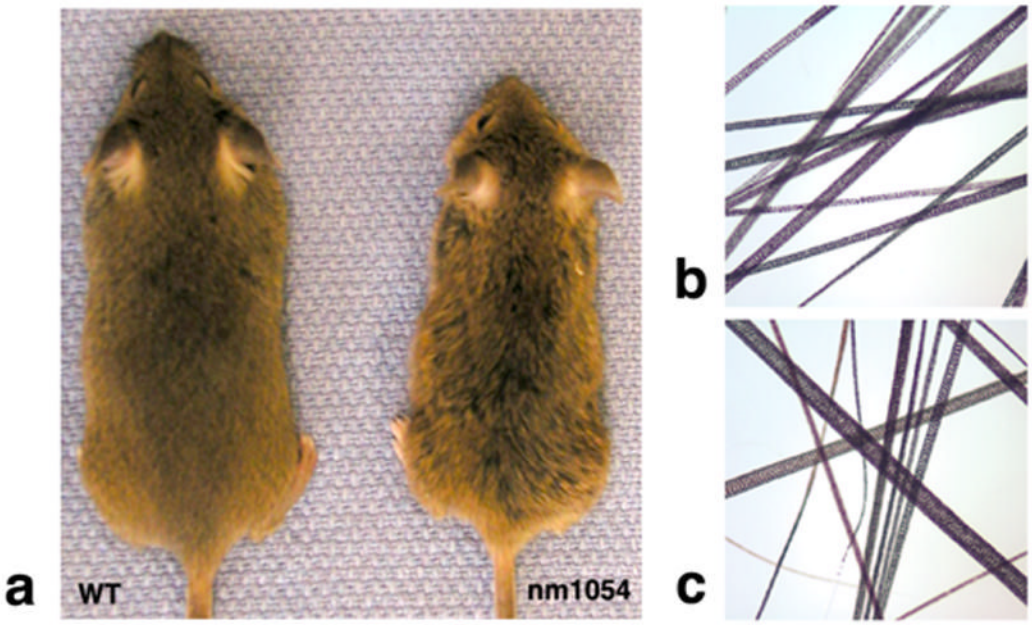

Figure 1. The *nm1054* hair phenotype

(**a**) Appearance of eight week, male, B6129F1 wild type (left) and *nm1054* deletion homozygous (right) mice. Note the matted, greasy appearance of the *nm1054* fur. (**b**) Hair from the back of an eight week, male, B6129F1 *nm1054* heterozygote. Magnification is 10X. (**c**) Hair from the back of an eight week, male, B6129F1 *nm1054* deletion homozygote. The mutant hair appears more reddish in color. Magnification is 10X.

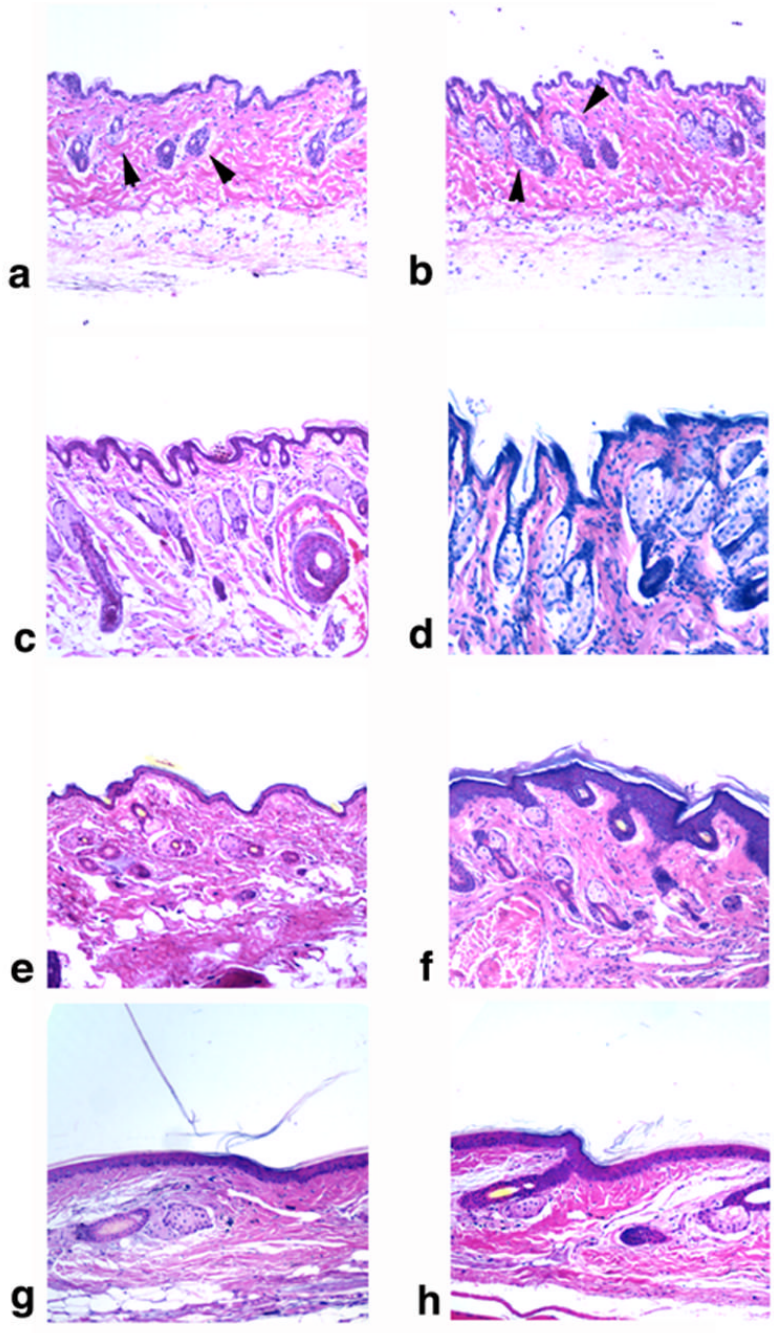

Figure 2. Histological analysis of skin from eight week, male, wild type and *nm1054* mice

(**a–b**) Sections of wild type (**a**) and *nm1054* (**b**) skin from the lower thorax. (**c–d**) Sections of wild type (**c**) and *nm1054* (**d**) skin from the nose. (**e–f**) Sections of wild type (**e**) and *nm1054* (**f**) skin from the paws. (**g–h**) Sections of wild type (**g**) and *nm1054* (**h**) skin from the tail. Arrowheads indicate pilosebaceous units (PSUs). Magnification is 10X. All sections are stained with hematoxylin and eosin.

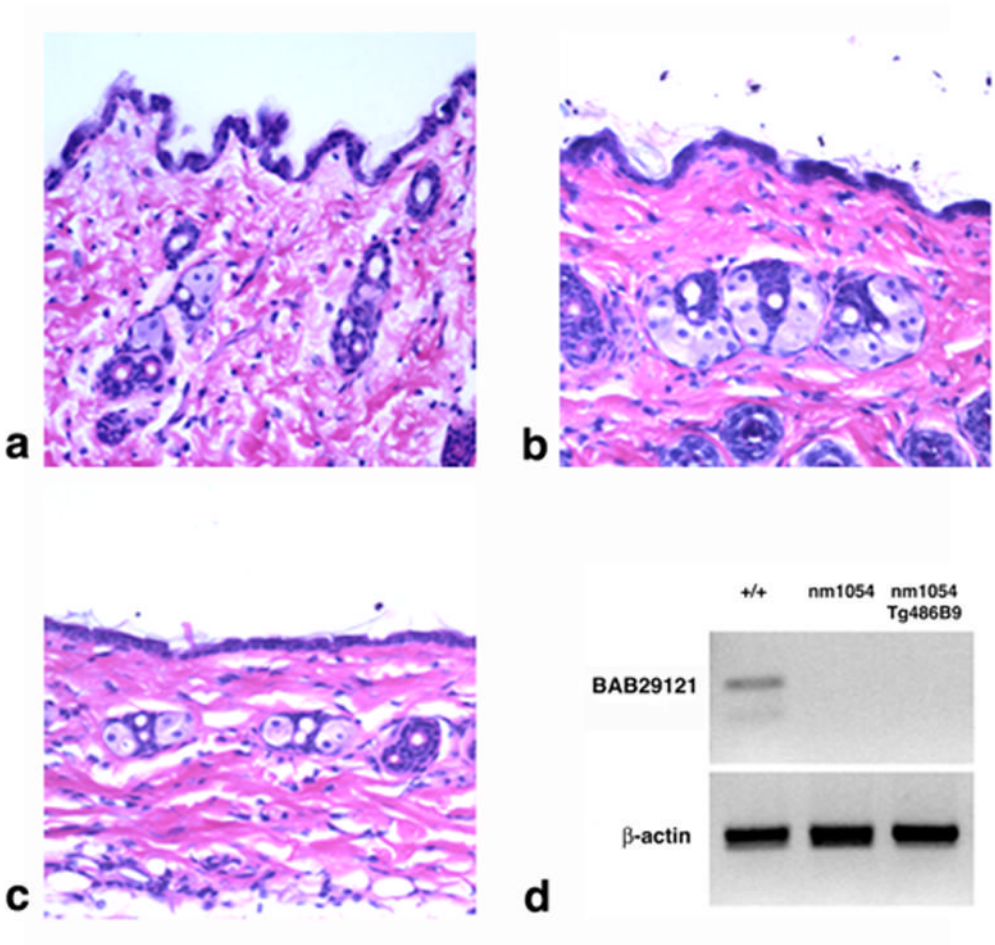

Figure 3. BAC transgenic rescue of the *nm1054* cutaneous abnormality

(**a–c**) Histology of wild type (**a**), *nm1054* (**b**), and BAC 486B9 transgenic *nm1054* (**c**) skin from the lower thorax. Magnification is 20X. All sections are stained with hematoxylin and eosin. (**d**) RT PCR of *BAB29121* from mouse thymus RNA. *β-actin* was used as a loading control.

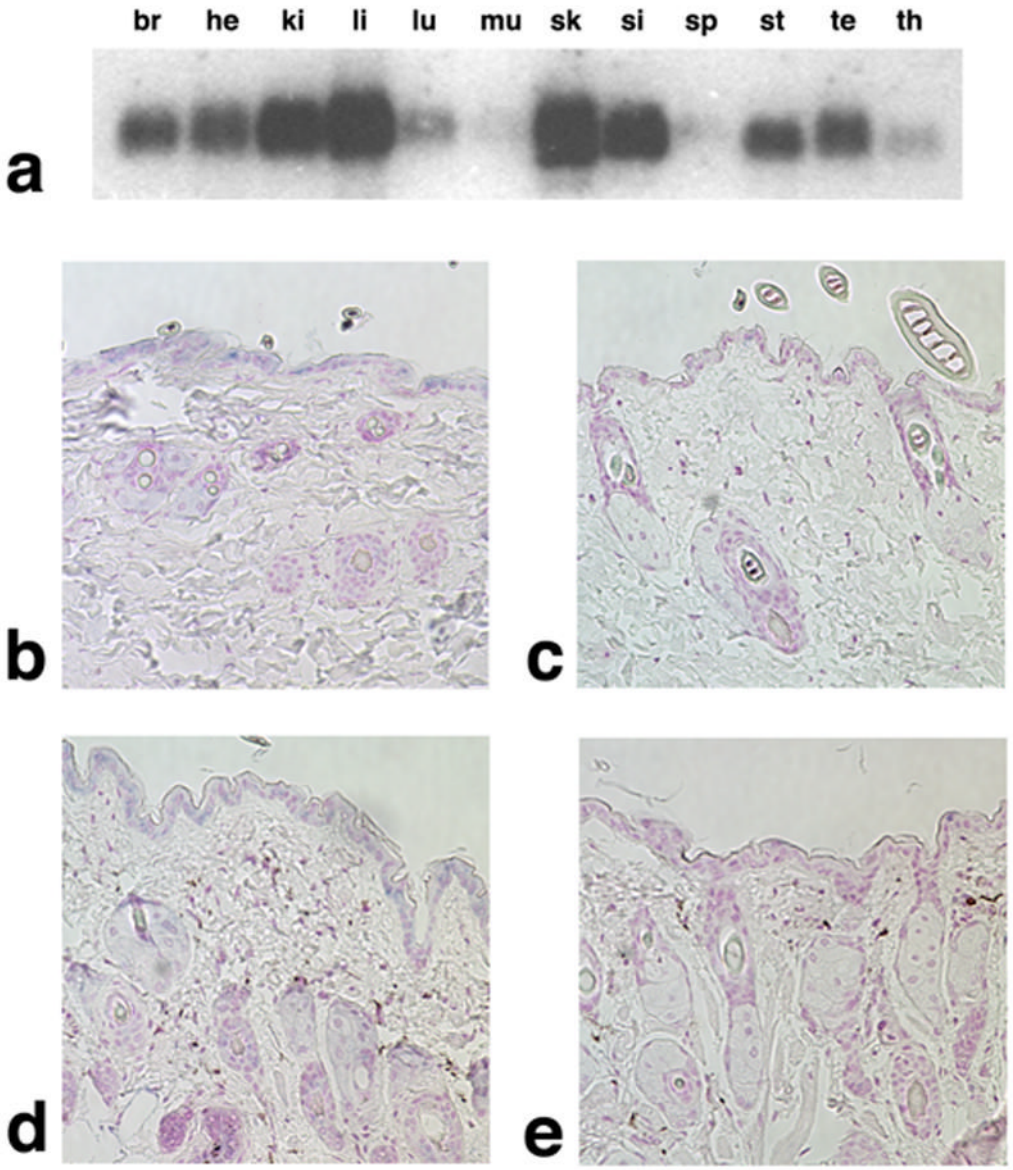

Figure 4. Expression of mouse *Acbp*

(**a**) Northern analysis of *Acbp* mRNA expression in brain (br), heart (he), kidney (ki), liver (li), lung (lu), muscle (mu), skin (sk), small intestine (si), spleen (sp), stomach (st), testis (te), and thymus (th). (**b–c**) *In situ* hybridization analysis of *Acbp* expression in eight week, male, wild type (**b**) and *nm1054* (**c**) mouse skin from the lower thorax. (**d–e**) *In situ* hybridization analysis of *Acbp* expression in eight week, male, wild type (**d**) and *nm1054* (**e**) mouse skin from the nose. Blue staining indicates *Acbp* expression in the epidermis, hair follicles, and sebocytes. Magnification is 20X.

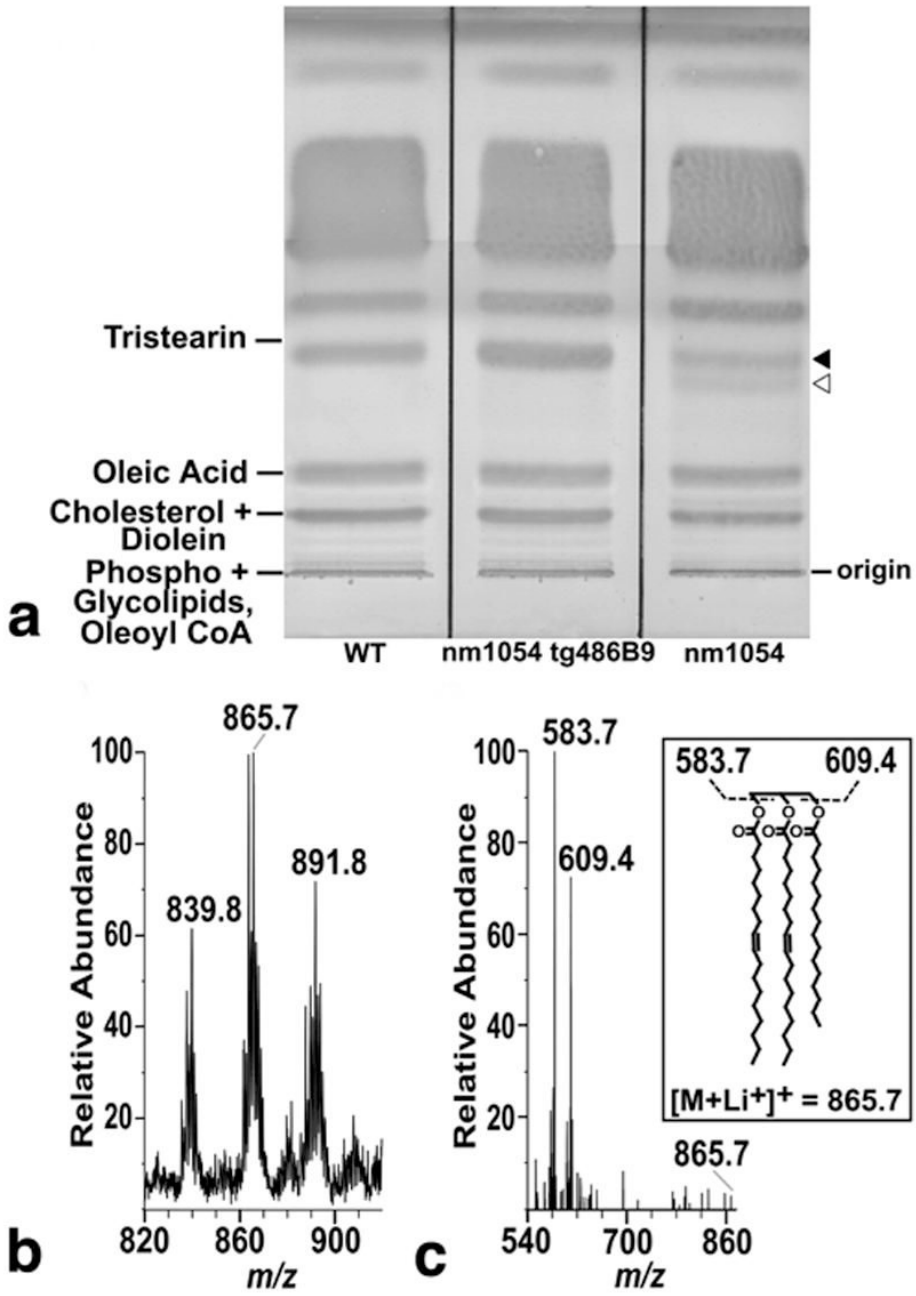

Figure 5. Chromatographic analysis of hair lipids

(**a**) Preparative silica TLC of lipids extracted from wild type, BAC 486B9 transgenic *nm1054*, and *nm1054* hair showing a lower intensity band (closed arrowhead) in the *nm1054* hair nearly co-migrating with a triacylglycerol standard (tristearin), as well as a unique band (open arrowhead) not present in wild type or transgenic mutant hair. (**b**) Positive mode mass spectrometric analysis with lithium of *nm1054* hair lipids indicated by the closed arrow in Figure 5a, yielding ions of *m/z* 839.8, 865.7, and 891.8. The ion at *m/z* 865.7 corresponds to the expected mass of a lithium adduct of a triacylglycerol. (**c**) Collision-induced mass spectrometry spectrum of the ion at *m/z* 865.7 shows product ions corresponding to lithium adducts of diacylglycerol units after the loss of $C_{18:1}$ (*m/z* 583.7) and $C_{16:0}$ (*m/z* 609.4),

confirming the initial structure of a triacylglycerol with two $C_{18:1}$ and one $C_{16:0}$ fatty acyl units (inset). The positions of fatty acids and unsaturations are shown arbitrarily.